Analysis of Hepatic Disposition of Galactosylated Cationic Liposome/Plasmid DNA Complexes in Perfused Rat Liver

Shintaro Fumoto,[1] Fumi Nakadori,[1] Shigeru Kawakami,[1] Makiya Nishikawa,[1] Fumiyoshi Yamashita,[1] and Mitsuru Hashida[1,2]

Received February 26, 2003; accepted May 14, 2003

Purpose. To determine the intrahepatic disposition characteristics of galactosylated liposome/plasmid DNA (pDNA) complexes in perfused rat liver.

Methods. Galactosylated liposomes containing N-[1-(2,3-dioleyloxy)propyl]-N,N,N-trimethylammonium chloride (DOTMA), cholesterol (Chol), and cholesten-5-yloxy-N-{4-[(1-imino-2-D-thiogalactosylethyl)amino]butyl} formamide (Gal-C4-Chol) were prepared. The liposome/[^{32}P]-labeled pDNA complexes were administered to perfused liver, and the venous outflow patterns were analyzed based on a two-compartment dispersion model.

Results. The single-pass hepatic extraction of pDNA complexed with DOTMA/Chol/Gal-C4-Chol liposomes was greater than that with control DOTMA/Chol liposomes. A two-compartment dispersion model revealed that both the tissue binding and cellular internalization rate were higher for the DOTMA/Chol/Gal-C4-Chol liposome complexes compared with the control liposome complexes. The tissue binding was significantly reduced by the presence of 20 mM galactose. When their cellular localization in the perfused liver at 30 min postinjection was investigated, it was found that the parenchymal uptake of the DOTMA/Chol/Gal-C4-Chol liposome complexes was greater than that of the control liposome complexes. The parenchymal cell/nonparenchymal cell uptake ratio was as high as unity.

Conclusion. Galactosylation of the liposome/pDNA complexes increases the tissue binding and internalization rate via an asialoglycoprotein receptor-mediated process. Because of the large particle size of the complexes (~150 nm), however, penetration across the fenestrated sinusoidal endothelium appears to be limited.

KEY WORDS: gene delivery; galactosylated liposomes; cationic liposomes; dispersion model.

INTRODUCTION

Gene delivery to hepatocytes is of great therapeutic potential because the cells are responsible for the synthesis of a wide variety of proteins that play important biologic roles both inside and outside the liver. So far, several *in vivo* (1–3) and *ex vivo* (4,5) methods have been investigated for the delivery of exogenous therapeutic genes to the liver. In a series of experiments, we have focused on receptor-mediated *in vivo* gene delivery to hepatocytes and developed several types of macromolecular (6,7) and particulate (8,9) gene carriers. Cationic liposomes containing cholesten-5-yloxy-N-{4-[(1-imino-2-D-thiogalactosyl-ethyl)amino]butyl} formamide (Gal-C4-Chol) are one potential carrier (8) that can efficiently be recognized by asialoglycoprotein receptors expressed exclusively in hepatocytes. This cholesterol derivative possesses a bifunctional molecular structure, i.e., an imino group for binding to pDNA via electrostatic interaction and a galactose residue for the cell surface receptors in hepatocytes. Therefore, a high density of galactose residues can be provided on the liposome surface without losing the ability to bind to pDNA, unlike other neutral molecules. We have demonstrated that Gal-C4-Chol-containing liposomes are effective for *in vivo* gene delivery (9) as well as *in vitro* delivery (8).

A number of possible barriers, from administration through gene expression, are associated with *in vivo* gene delivery (10–12). Detailed information on these barrier properties is needed for the rational design of effective gene carriers. *In vitro* experiments have been carried out to quantitatively or visually characterize cellular uptake or subcellular transport of exogenous genes complexed with their carrier systems. Although *in vitro* data give useful information about the optimization of the intracellular fate of delivery systems, it appears to be more critical to control their disposition at the whole-body level. Therefore, we have extensively studied the pharmacokinetics of naked pDNA (13) or that complexed with carriers systems (6,9,14) as well as carrying out *in vitro* studies (8,15). When pDNA complexed with Gal-C4-Chol liposomes was injected into the portal vein of mice, most of the amount injected was taken up by the liver during a single passage. The hepatic uptake of pDNA complexed with galactosylated liposomes was significantly higher than that with conventional cationic liposomes and closely correlated with gene expression experiments (9). However, the level of gene expression as a result of the galactosylated liposome/pDNA complexes was not as high as that expected from the *in vitro* results. There must be several barriers associated intrinsically with *in vivo* situations, such as convective blood flow in the liver, passage through the sinusoids, and tissue interactions. Unfortunately, the *in vivo* distribution study of radiolabeled pDNA is not precise enough to determine the characteristics of these barriers.

Alternatively, a single-pass liver perfusion experiment appears to be suitable for this purpose. We have already used a rat liver perfusion system to determine the hepatic disposition characteristics of low-molecular-weight drugs, macromolecules, and drug carrier systems (16–19). When [^{32}P]-labeled naked pDNA is injected into the isolated perfused liver, it is extensively taken up by the liver, and the uptake obeys saturable kinetics (20). Moreover, the total recovery of naked pDNA in the liver was reduced substantially by preadministration of polyinosinic acid, dextran sulfate, succinylated bovine serum albumin, but not by polycytidylic acid, suggesting that pCAT is taken up by the liver via scavenger receptors for polyanions on the NPC. Thus, a liver perfusion system

[1] Department of Drug Delivery Research, Graduate School of Pharmaceutical Sciences, Kyoto University, Sakyo-ku, Kyoto 606-8501, Japan.

[2] To whom correspondence should be addressed. (e-mail: hashidam@pharm.kyoto-u.ac.jp)

ABBREVIATIONS: DOTMA, N-[1-(2,3-dioleyloxy)propyl]-N,N,N-trimethylammonium chloride; Chol, cholesterol; Gal-C4-Chol, cholesten-5-yloxy-N-{4-[(1-imino-2-D-thiogalactosylethyl)amino]butyl}formamide; PC, parenchymal cells; NPC, nonparenchymal cells; BSA, bovine serum albumin; k_{12}, forward partition rate constants; k_{21}, backward partition rate constants; k_{int}, internalization rate constant; D_C, corrected dispersion coefficient; V_S, sinusoidal volume; D_N, dispersion number.

0724-8741/03/0900-1452/0 © 2003 Plenum Publishing Corporation

allowed us to determine the uptake characteristics of various molecules and complexes with the structure of the liver intact.

In the present study, we investigated the local disposition of liposome/pDNA complexes using a single-pass rat liver perfusion system. The venous outflow profile of the complexes following a bolus input into the isolated perfused liver was analyzed by a two-compartment dispersion model to quantitatively evaluate the difference in each kinetic process between conventional cationic liposome complexes and galactosylated liposome complexes. Here, N-[1-(2,3-dioleyloxy)propyl]-N,N,N-trimethylammonium chloride (DOTMA)/cholesterol (Chol) liposomes were selected as model cationic liposomes, which are known to have a high *in vivo* gene transfection activity (21).

MATERIALS AND METHODS

Materials

N-(4-Aminobutyl)carbamic acid *tert*-butyl ester and DOTMA were obtained from Tokyo Chemical Industry Co. Ltd. (Tokyo, Japan). [α-^{32}P]dCTP (3000 Ci/mmole) was obtained from Amersham (Tokyo, Japan). Chol and Clear-Sol I were obtained from Nacalai Tesque (Kyoto, Japan), and Soluene 350 was purchased from Packard (Groningen, Netherlands). Cholesteryl chloroformate and collagenase type IA were obtained from Sigma Chemicals Inc. (St. Louis, MO, USA). Diethylenetriaminepentaacetic acid (DTPA) anhydride was purchased from Dojindo Laboratory (Kumamoto, Japan). Indium-111 chloride ([^{111}In]$InCl_3$) was supplied by Nihon Medi-Physics Co. (Hyogo, Japan). Bovine serum albumin (BSA) was radiolabeled with ^{111}In using DTPA anhydride as reported previously (22). All other chemicals were of the highest purity available.

Construction and Preparation of pDNA

pCMV-Luc was constructed by subcloning the Hind III/Xba I firefly luciferase cDNA fragment from pGL3-control vector (Promega, Madison, WI, USA) into the polylinker of pcDNA3 vector (Invitrogen, Carlsbad, CA, USA). pDNA was amplified in the *E. coli* strain DH5α, isolated, and purified using a Qiagen Endofree Plasmid Giga Kit (Qiagen GmbH, Hilden, Germany). Purity was confirmed by 1% agarose gel electrophoresis followed by ethidium bromide staining, and the DNA concentration was measured by UV absorption at 260 nm. The pDNA was labeled with [α-^{32}P]dCTP by nick translation (23).

Synthesis of Gal-C4-Chol

Gal-C4-Chol was prepared as reported previously (8). Cholesteryl chloroformate and N-(4-aminobutyl)carbamic acid *tert*-butyl ester were reacted in chloroform for 24 h at room temperature. A solution of trifluoroacetic acid and chloroform was added dropwise, and the mixture was stirred for 4 h at 4°C. The solvent was evaporated to obtain N-(4-aminobutyl)-(cholesten-5-yloxyl)formamide, which was then combined with 2-imino-2-methoxyethyl-1-thiogalactoside (24), and the mixture was stirred for 24 h at room temperature. After evaporation, the resultant material was suspended in water, dialyzed against distilled water for 48 h (12 kDa cutoff dialysis tubing), and then lyophilized.

Preparation of Cationic Liposomes

Mixtures of Gal-C4-Chol, DOTMA, and Chol were dissolved in chloroform, vacuum-desiccated, and resuspended in sterile 5% dextrose at a concentration of 4 mg/ml total lipids. The molar ratios of lipids were 1:1 for DOTMA/Chol liposomes and 1:0.5:0.5 for DOTMA/Chol/Gal-C4-Chol, respectively. The suspension was sonicated for 3 min, and the resulting liposomes were extruded 10 times through double-stacked 100-nm polycarbonate membrane filters.

Preparation of Cationic Liposome/pDNA Complexes

Nine hundred microliters of 200 μg/ml pDNA in 5% dextrose was mixed with an equal volume of cationic liposomes varying in their concentrations (250 to 3100 μg/ml) and incubated for 30 min at room temperature. The mixing ratio of liposomes and pDNA was expressed as a +/– charge ratio, which is the molar ratio of cationic lipids to pDNA phosphate residue (10). The charge ratio of unity was 3.26 μg total lipid/μg pDNA in the case of DOTMA/Chol liposomes and 2.52 μg total lipid/μg pDNA in the case of DOTMA/Chol/Gal-C4-Chol liposomes, respectively. The particle size and zeta potential of the cationic liposome/pDNA complexes were measured, using a dynamic light-scattering spectrophotometer (LS-900, Otsuka Electronics, Osaka, Japan) and a laser electrophoresis zeta-potential analyzer (LEZA-500T, Otsuka Electronics), respectively.

Liver Perfusion Experiment

Male Wistar rats (170–210 g) were purchased from the Shizuoka Agricultural Cooperative Association for Laboratory Animals (Shizuoka, Japan). All animal experiments were carried out in accordance with the Principles of Laboratory Animal Care as adopted and promulgated by the U.S. National Institutes of Health and the Guideline for Animal Experiments of Kyoto University.

In situ liver perfusion studies were carried out as reported previously (16). Rats were anesthetized by intraperitoneal injection of sodium pentobarbital (60 mg/kg). The portal vein was catheterized with a polyether nylon catheter (Surflo® IV Catheter, 16 G×2″, Terumo, Tokyo, Japan) and immediately perfused with Krebs-Ringer bicarbonate buffer supplemented with 10 mM glucose (oxygenated with 95% O_2–5% CO_2, adjusted to pH 7.4 at 37°C). The inferior vena cava was catheterized through the right atrium with a polyethylene tube (PE-160) and also ligated immediately above the renal vein. The perfusate was circulated using a peristaltic pump (SJ-1211, ATTO Co., Tokyo, Japan) at a flow rate of 13 ml/min. After a stabilization period of 25 min, liposome/[^{32}P]pDNA complexes (30 μg DNA/300 μl) were administered to the portal vein using a six-position rotary valve injector (Type 50 Teflon rotary valves, Rheodyne Inc., Cotati, CA, USA). Samples of venous outflow were collected into the preweighed tubes, and the volumes were estimated from the weight gain. The sampling time was calculated from each sample volume, assuming a constant flow rate. The lag time of the catheter between the injector and the liver was estimated from the catheter volume and flow rate. After completion of the perfusion experiment, the entire liver was excised, weighed, and homogenized. The radioactivity of the effluent perfusate was measured in a scintillation counter (LSA-500,

Beckman, Tokyo, Japan) after addition of 5 ml Clear-Sol I. The radioactivity of liver homogenates was measured after incubation with Soluene-350 overnight at 45°C and mixing with 0.2 ml isopropanol, 0.2 ml 30% hydrogen peroxide, 0.1 ml 5 N HCl, and 5 ml Clear-Sol I in that order.

Pharmacokinetic Analysis

The outflow patterns were analyzed by statistical moment analysis for local injection as reported previously (25). Briefly, the area under the curve (AUC) and mean residence time (MRT) were calculated as follows:

$$AUC = \int_0^\infty C dt \tag{1}$$

$$MRT = \int_0^\infty tCdt/AUC \tag{2}$$

where t is the time and C is the concentration of [^{32}P]pDNA complexed with cationic liposomes. The moments can be calculated by numerical integration using a linear trapezoidal formula and extrapolation to infinite time based on a monoexponential equation (26). The t values were corrected for the lag time of the catheter. The recovery ratio (F) and extraction ratio (E) were derived from F = AUC · Q (flow rate) and E = 1 – F, respectively.

The outflow patterns were also analyzed based on a two-compartment dispersion model, where sinusoidal and binding compartments were considered as shown in Fig. 1. The mass balance equations involving the axial dispersion in the sinusoidal space are given as follows (27):

$$\frac{\partial C_S(t,z)}{\partial t} + v\frac{\partial C_S(t,z)}{\partial z} = D\frac{\partial^2 C_S(t,z)}{\partial z^2} - k_{12}\cdot C_S(t,z) + \varepsilon k_{21}\cdot C_B(t,z) \tag{3}$$

$$\frac{\partial C_B(t,z)}{\partial t} = \frac{1}{\varepsilon}k_{12}\cdot C_S(t,z) - k_{21}\cdot C_B(t,z) - k_{int}\cdot C_B(t,z) \tag{4}$$

where $C_S(t,z)$ and $C_B(t,z)$ are the concentration of drug in the sinusoidal space and binding compartment, respectively; D is the dispersion coefficient; ε is the volume ratio of the binding compartment to the sinusoidal space in the liver; k_{12} and k_{21} are the forward and backward partition rate constants between the sinusoidal space and binding compartment; k_{int} is the first-order internalization rate constant from the binding compartment to the intracellular space; v is the linear flow velocity of the perfusate; t is time; and z is the axial coordinate in the liver. The initial and boundary conditions are given as:

$$C_S(t,0) = M/Q\cdot f_I(t),\ C_S(0,z) = 0,\ C_S(t,\infty) = 0,$$
$$C_B(t,0) = 0,\ C_B(0,z) = 0$$

where M is the amount of drug injected into the liver, and Q is the flow rate of the perfusate; $f_I(t)$ has the dimension of the reciprocal of time. Taking the Laplace transform with respect to t, rearranging, replacing the length of the sinusoidal space L with z, and introducing the cross-sectional area of the sinusoidal space A, the following image equation is obtained:

$$\tilde{C}_S(s) = \frac{M}{Q}\tilde{f}_I(s)\cdot\exp\left[\left\{\frac{Q}{2D_C} - \sqrt{\left(\frac{Q}{2D_C}\right)^2 + \frac{1}{D_C}\left\{s + k_{12} - \frac{k_{12}\cdot k_{21}}{s + k_{21} + k_{int}}\right\}}\right\}V_S\right] \tag{5}$$

where $C_S(s)$ and $f_I(s)$ denote the Laplace transform of concentration in the venous outflow and input function $f_I(t)$, respectively. D_C is the corrected dispersion coefficient ($D_C = D\cdot A^2$), V_S is the sinusoidal volume (= L · A), and the flow rate Q is equal to A · v.

Each parameter (D_C, k_{12}, k_{21}, k_{int}, and V_S) was calculated by curve fitting of the Laplace-transformed equation to the experimental venous outflow pattern using a nonlinear least-squares program with a fast inverse Laplace transform algorithm MULTI (FILT) (28). The damping Gauss Newton method with no constraint was used for curve fitting the MULTI algorithm. Here, $f_I(t)$ was assumed to be a delta function because the liposome/pDNA complexes were rapidly injected using a six-rotary valve injector.

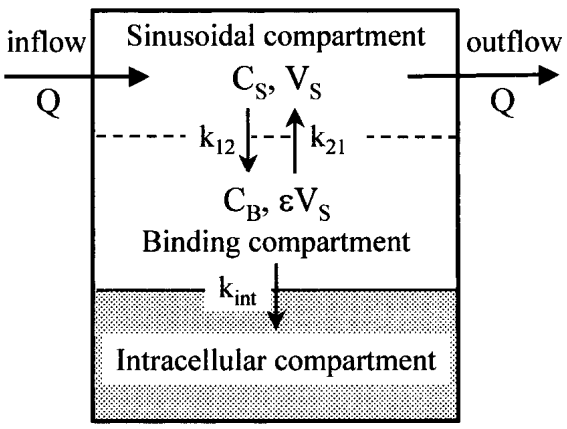

Fig. 1. A flow model for analyzing the hepatic disposition of cationic liposome/pDNA complexes. Q, flow rate (ml/min); C_S, sinusoidal concentration (% of dose/ml); V_S, sinusoidal volume (ml); C_B, concentration in the binding compartment; ε, volume ratio of the binding compartment to the sinusoidal compartment; k_{12}, association rate constants (min^{-1}); k_{21}, dissociation rate constants (min^{-1}); k_{int}, internalization rate constant (min^{-1}),

Cellular Localization of Liposome/[^{32}P]pDNA Complexes in Liver

Thirty minutes after injection of liposome/pDNA complexes into the isolated perfused liver, the perfusate was changed to Ca^{2+}-free buffer (Hepes solution, pH 7.2). Ten minutes later, the perfusate was switched to Hepes solution containing 5 mM $CaCl_2$ and 0.05% (w/v) collagenase (type IA, pH 7.5) and perfused for 10 min. Then, the cells were dispersed in ice-cold Hank's-Hepes buffer by gentle stirring and separated into parenchymal cells (PC) and nonparenchymal cells (NPC) by centrifugation as described previously (29). The number and viability of the cells were determined by the trypan blue exclusion method (30).

Statistical Analysis

Statistical comparisons were performed by Student's *t* test for two groups, one-way ANOVA for multiple groups, and Scheffe's *post hoc* test after ANOVA.

RESULTS AND DISCUSSION

Uptake of Liposome/pDNA Complexes by Perfused Rat Liver

Figure 2 shows typical venous outflow profiles of liposome/[^{32}P]pDNA complexes following bolus injection into

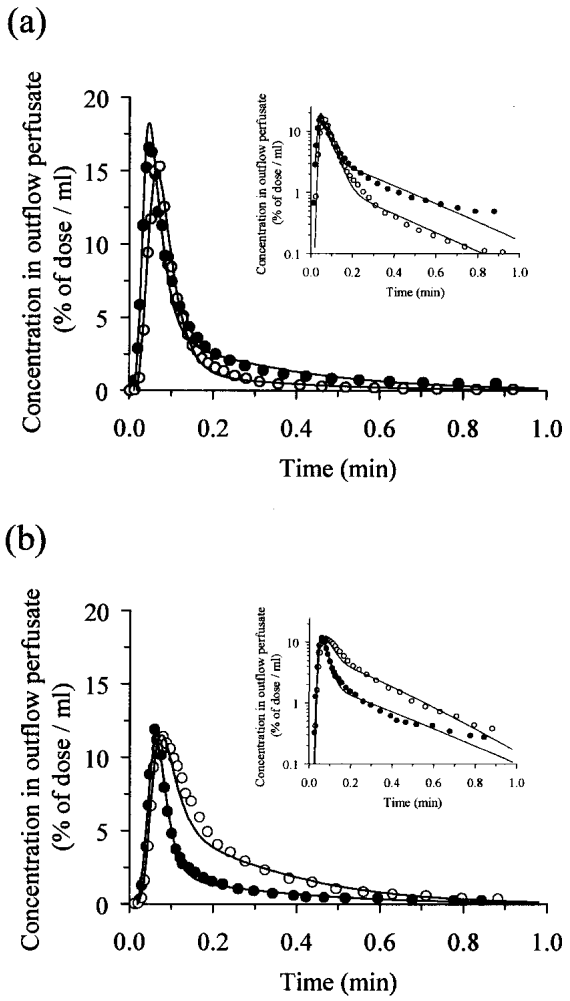

Fig. 2. Typical venous outflow patterns of [^{32}P]pDNA complexed with DOTMA/Chol (a) and DOTMA/Chol/Gal-C4-Chol (b) at a charge ratio of 2.3:1.0 following bolus injection into perfused rat liver. The insets show semilogarithmic plots. (●) and (○) represent the absence and presence of 20 mM galactose in the perfusate. The curves simulated by a two-compartment dispersion model are also shown in these figures.

the perfused rat liver. The maximum outflow concentration of Gal-C4-Chol-containing liposome/pDNA complexes (Fig. 2b) was lower than that of DOTMA/Chol liposome/pDNA complexes (Fig. 2a). The presence of 20 mM galactose in the perfusate markedly increased the venous outflow concentration of Gal-C4-Chol-containing liposome/pDNA complexes but not DOTMA/Chol liposome/pDNA complexes.

Moment analysis was performed to quantitatively describe the outflow pattern. The AUC value of DOTMA/Chol/Gal-C4-Chol complexes was smaller than that of DOTMA/Chol complexes, and the MRT value of DOTMA/Chol/Gal-Chol complexes was also smaller (Table I). When the radioactivity associated with the liver at 30-min postinjection was measured, it was found to be 50.8 ± 3.40% and 72.5 ± 2.23% for DOTMA/Chol and DOTMA/Chol/Gal-C4-Chol complexes, respectively.

Analysis Based on a Two-Compartment Dispersion Model

To characterize each kinetic process in the hepatic uptake of liposome/pDNA complexes, their outflow profiles were analyzed based on a two-compartment dispersion model (Fig. 1). As shown in Fig. 2, the simulation curves using the model were in good agreement with the observed data. Table II summarizes the parameters obtained by curve fitting to the observed data. Assuming that liposome/pDNA complexes are bound to the tissue surface and internalized (or sequestrated) into the liver, the k_{12}/k_{21} value represents a binding affinity to the liver tissue, while the k_{int} value represents the efficiency of internalization of tissue-bound liposome/pDNA complexes. The k_{12}/k_{21} value of Gal-C4-Chol containing liposome/pDNA complexes was twofold higher than that of DOTMA/Chol liposome/pDNA complexes, whereas the k_{int} value of the former was 1.3-fold higher than that of the latter. Addition of 20 mM galactose to the perfusate decreased the k_{12}/k_{21} value of Gal-C4-Chol-containing liposome/pDNA complexes up to one-third, suggesting that asialoglycoprotein receptor-mediated endocytosis was involved in the hepatic disposition of Gal-C4-Chol-containing liposomes/pDNA complexes. Because DOTMA/Chol liposome/pDNA complexes appeared to bind to the tissues via multivalent electrostatic interactions, the tissue binding would be relatively strong. Therefore, it should be noted that Gal-C4-Chol-

Table I. Moment Parameters for Liposome/[^{32}P]pDNA Complexes in the Liver Perfusion Experiments

	AUC (% of dose · s/ml)	MRT (s)	E (%)
Without galactose			
DOTMA/Chol	135.0 ± 13.0	20.5 ± 4.99	71.3 ± 2.89
DOTMA/Chol/Gal-C4-Chol	76.7 ± 13.0**	11.9 ± 1.68*	83.8 ± 2.77**
With 20 mM galactose			
DOTMA/Chol	96.3 ± 2.40$^{\#\#}$	24.3 ± 14.1	79.7 ± 1.00$^{\#\#}$
DOTMA/Chol/GAl-C4-Chol	151.4 ± 42.7$^{\#}$	15.9 ± 2.46	69.2 ± 6.82$^{\#}$

Results are expressed as the mean ± SD of three experiments.
Extraction ratios (E) were calculated as follows: E = 1 – AUC · Q (flow rate).
Significant differences compared with DOTMA/Chol control group (*$p < 0.05$, **$p < 0.01$).
Significant differences compared with correspondent control group ($^{\#}p < 0.05$, $^{\#\#}p < 0.01$).

Table II. Pharmacokinetic Parameters and Inhibition Effect for Hepatic Disposition of Liposome/[^{32}P]pDNA Complexes Analyzed by Two-Compartment Dispersion Model

	Rate constants				Other parameters			
	k_{12} (min^{-1})	k_{21} (min^{-1})	k_{12}/k_{21}	k_{int} (min^{-1})	D_c ($ml^2 min$)	V_S (ml)	D_N	V_S/g liver
DOTMA/Chol complexes								
Control	26.1 ± 0.57	2.07 ± 0.22	12.7 ± 1.19	2.82 ± 0.24	3.01 ± 0.60	1.39 ± 0.07	0.17 ± 0.03	0.21 ± 0.02
+ Galactose	21.0 ± 3.32	0.63 ± 0.07$^{\#\#}$	33.7 ± 8.58$^{\#}$	3.79 ± 0.27$^{\#\#}$	2.80 ± 0.60	1.58 ± 0.20	0.14 ± 0.02	0.20 ± 0.02
DOTMA/Chol/Gal-C4-Chol complexes								
Control	30.0 ± 0.13**	1.23 ± 0.23**	24.9 ± 4.41**	3.77 ± 0.46*	1.94 ± 0.40	1.29 ± 0.10	0.12 ± 0.02	0.20 ± 0.03
+Galactose	19.7 ± 3.80$^{\#\#}$	2.92 ± 1.20	7.38 ± 2.28$^{\#\#}$	3.51 ± 0.23	2.73 ± 0.52	1.65 ± 0.29	0.14 ± 0.06	0.22 ± 0.05

Results are expressed as the mean ± SD of three experiments.
Significant differences compared with DOTMA/Chol control group (* $p < 0.05$, ** $p < 0.01$).
Significant differences compared with correspondent control group ($^{\#}$ $p < 0.05$, $^{\#\#}$ $p < 0.01$).

containing liposome/pDNA complexes exhibited higher tissue binding than DOTMA/Chol liposome/pDNA complexes. It is known that asialoglycoprotein receptors recognize galactose moieties of the substrate multivalently (31–33). Although Gal-C4-Chol itself has only one sugar residue, galactosylated liposome/pDNA complexes could interact multivalently with the receptor when the concentration of galactose residues on the liposome surface is high enough. This hypothesis is a reasonable one because Gal-C4-Chol accounts for one-fourth of the total lipids in our galactosylated liposomes.

In this analysis, five intrinsic parameters were estimated by curve fitting to a single outflow pattern. However, the reliability of estimated parameters would be guaranteed by their small standard deviation. In addition, the volume of the sinusoidal space (V_S) was almost constant in all the experiments (Table II). When the outflow profile of [^{111}In]BSA that little interacts with tissue was analyzed based on a two-compartment dispersion model where the k_e equals zero, the V_S value was estimated to be 0.21 ± 0.05 ml/g tissue. Thus, this consistency in the physiologic parameter suggests the validity of the present model.

When the venous outflow pattern of naked [^{32}P] pDNA was analyzed by the two-compartment dispersion model (raw data not shown), the k_{12}/k_{21} and k_{int} values were 2.07 ± 1.28 and 2.64 ± 0.26 min^{-1}, respectively. Comparison with the k_{12}/k_{21} values of the liposome/pDNA complexes (i.e., 12.7 ± 1.19 and 24.9 ± 4.41 for DOTMA/Chol and DOTMA/Chol/Gal-C4-Chol complexes, respectively) indicated that complexation with these liposomes greatly enhanced the tissue-binding of pDNA.

Effect of Charge Ratio on Hepatic Cellular Uptake

The cationic charge of liposome/pDNA complexes is known to be an important factor affecting their biodistribution, transfection efficiency, and stability (9,10,12,34), whereas the Gal-C4-Chol content of liposomes has a minute effect on transfection efficiency *in vivo* (9) as well as *in vitro* (8). Accordingly, we evaluated the effect of charge ratio on hepatic disposition of liposome/pDNA complexes.

Figure 3a shows typical venous outflow patterns of [^{32}P] pDNA complexed with DOTMA/Chol liposomes. Although the outflow pattern was similar for both the 2.3:1.0 and 4.7:1.0 complexes, the peak concentration of the outflow patterns for

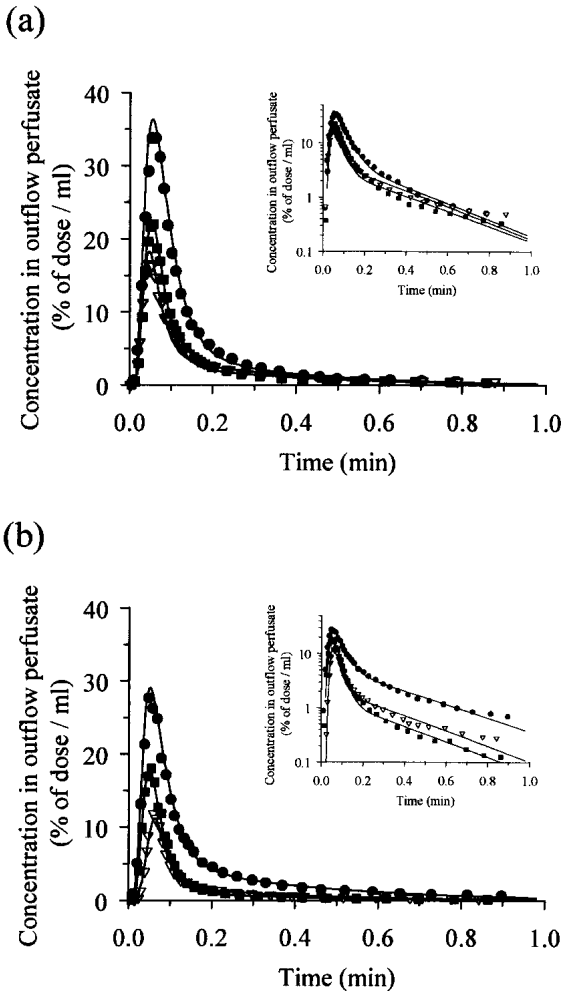

Fig. 3. Typical venous outflow patterns of [^{32}P]pDNA complexed with DOTMA/Chol (a) and DOTMA/Chol/Gal-C4-Chol (b) at various charge ratios following bolus injection into perfused rat liver. The insets show semilogarithmic plots. Cationic liposomes were complexed with [^{32}P]pDNA at charge ratios of 0.5:1.0 (●), 2.3:1.0 (▽), and 4.7:1.0 (■), respectively. The curves simulated by a two-compartment dispersion model are also shown in these figures.

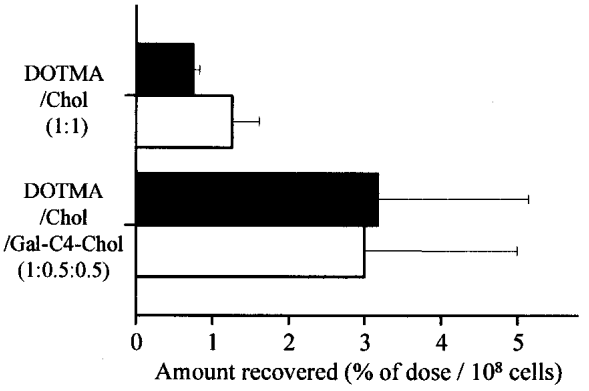

Fig. 4. Hepatic cellular localization of liposome/[^{32}P]pDNA (30 μg) complexes at a charge ratio of 2.3:1.0 following bolus injection into perfused rat liver. Filled and open bars represent PC and NPC. Each value is expressed as the mean ± SD of three experiments.

the 0.5:1.0 complexes was markedly higher. When the outflow patterns of the DOTMA/Chol liposome/pDNA complexes were analyzed based on a two-compartment dispersion model (Table III, upper), it was found that the k_{12}/k_{21} ratio was significantly smaller for the 0.5:1.0 complexes, whereas the k_{int} was almost the same irrespective of the charge ratio of the complexes. As for the DOTMA/Chol liposome complexes, the k_{12}/k_{21} ratio was closely related to their zeta potential (Table III). Thus, it was confirmed that the surface charge density of the complexes is an important factor determining the tissue binding of the liposome/pDNA complexes.

As for the DOTMA/Chol/Gal-C4-Chol complexes with a charge ratio of 0.5:1.0, the outflow concentration was higher than that for the 2.3:1.0 and 4.7:1.0 complexes (Fig. 3b). Analysis by a two-compartment dispersion model (Table III, lower) revealed that the k_{12}/k_{21} ratios and the k_{int} for the 2.3:1.0 and 4.7:1.0 complexes were markedly greater than those for the 0.5:1.0 complexes. When the DOTMA/Chol/Gal-C4-Chol complexes were compared with the corresponding DOTMA/Chol complexes, significant differences in k_{12}/k_{21} and k_{int} were observed with the 2.3:1.0 and 4.7:1.0 complexes but not with the 0.5:1.0 complexes. In addition, the zeta potential of the DOTMA/Chol/Gal-C4-Chol liposome complexes at a charge ratio of 0.5:1.0 was negative. These results suggest that a sufficient number of the galactose moieties in the complexes at charge ratio of 0.5:1.0 do not protrude from the surface of the complexes.

Cellular Distribution of Liposome/pDNA Complexes

The cellular distribution of liposome/[^{32}P] complexes was investigated following bolus injection into perfused rat liver (Fig. 4). When the radioactivities associated with liver parenchymal cells (PC) and nonparenchymal cells (NPC) per unit cell number were measured, the PC/NPC ratio for the DOTMA/Chol/Gal-C4-Chol liposome/pDNA complexes was 1.06, which was higher than that for the DOTMA/Chol liposome/pDNA complexes (0.59). In populations of parenchymal cells and nonparenchymal cells in rat liver (35), the parenchymal and nonparenchymal uptake of DOTMA/Chol/Gal-C4-Chol liposome/pDNA complexes was estimated to be 56.2% and 27.6% of the dose, respectively. As for DOTMA/Chol liposomes, 37.8% and 33.5% of the dose were taken up by parenchyma and nonparenchyma, respectively. Thus, the parenchymal uptake was marked for the DOTMA/Chol/Gal-C4-Chol complexes compared to DOTMA/Chol complexes.

However, the PC uptake of both DOTMA/Chol and DOTMA/Chol/Gal-C4-Chol complexes was not as high as expected from the surface area of parenchyma. The parenchyma is known to occupy 73% of the surface area of the liver plasma membrane (36). We have previously reported that cationic macromolecules distribute in both PC and NPC in proportion to their surface areas (17). However, unlike macromolecules, which can freely penetrate the sinusoidal endothelium through their large fenestrae [100–200 nm in diameter (37–39)], penetration of the liposome/pDNA complexes would be greatly limited. The mean particle sizes of DOTMA/Chol and DOTMA/Chol/Gal-C4-Chol liposome/pDNA complexes at a charge ratio of 2.3:1.0 were 137.7 ± 25.7 nm and 141.1 ± 6.5 nm (n = 3) (9), which are comparable with the size of the sinusoidal fenestrae. Restricted penetration across the sinusoidal endothelium would result in lower PC uptake of liposome/pDNA complexes. We have already optimized the particle sizes of liposome/pDNA complexes (9). To improve the efficacy of delivery of pDNA with galactosylated liposomes, however, the size of the complexes must be reduced further by some means.

Table III. Effect of Charge Ratio on Pharmacokinetic Parameters for Hepatic Disposition of Liposome/[^{32}P]pDNA Complexes Analyzed by Two-Compartment Dispersion Model

		Rate constants				Other parameters			
Charge ratio (+:−)	ζPotential (mV)	k_{12} (min^{-1})	k_{21} (min^{-1})	k_{12}/k_{21}	k_{int} (min^{-1})	D_c (ml^2min)	V_S (ml)	D_N	V_s/g liver
DOTMA/Chol complexes									
0.5:1.0	−34.6 ± 1.14	11.0 ± 1.67**	1.55 ± 0.31	7.47 ± 2.83	2.88 ± 0.11	3.92 ± 0.08	1.49 ± 0.01	0.21 ± 0.004	0.20 ± 0.01
2.3:1.0	35.1 ± 1.04	26.1 ± 0.57	2.07 ± 0.22	12.7 ± 1.19	2.82 ± 0.24	3.01 ± 0.60	1.39 ± 0.07	0.17 ± 0.03	0.21 ± 0.02
4.7:1.0	34.2 ± 3.48	18.3 ± 3.46*	1.15 ± 0.28*	16.0 ± 1.24	2.43 ± 0.52	2.66 ± 0.60	1.49 ± 0.17	0.15 ± 0.03	0.24 ± 0.02
DOTMA/Chol/Gal-C4-Chol complexes									
0.5:1.0	−29.8 ± 2.10	13.0 ± 0.95**	2.24 ± 0.13**	5.84 ± 0.73*	2.14 ± 0.15*	3.95 ± 0.96	1.67 ± 0.10	0.19 ± 0.06	0.25 ± 0.01
2.3:1.0	34.7 ± 0.35	30.0 ± 0.13	1.23 ± 0.23	24.9 ± 4.41	3.77 ± 0.46	1.94 ± 0.40	1.29 ± 0.10	0.12 ± 0.02	0.20 ± 0.03
4.7:1.0	34.8 ± 1.73	23.6 ± 1.59**	0.93 ± 0.16	25.7 ± 4.10	3.96 ± 0.64	3.13 ± 0.32	1.40 ± 0.09	0.17 ± 0.02	0.18 ± 0.03

Results are expressed as the mean ± SD of three experiments.
Significant differences compared with corresponding charge ratio 2.3 group (* $p < 0.05$, ** $p < 0.01$).

CONCLUSIONS

We have determined the hepatic disposition characteristics of DOTMA/Chol liposome and DOTMA/Chol/Gal-C4-Chol liposome/pDNA complexes using perfused rat liver, demonstrating that both tissue binding and cellular internalization were enhanced by galactosylation of the cationic liposomes. For the DOMTA/Chol/Gal-C4-Chol liposome/pDNA complexes to be effectively taken up by the liver, i.e., enough liposome pDNA, the charge ratio of 2.3:1.0 is necessary. These findings provide useful information for the rational design of targeted gene delivery systems to the liver parenchymal cells via asialoglycoprotein receptors.

ACKNOWLEDGMENT

This work was supported in part by Grants-in-Aid for Scientific Research from the Ministry of Education, Culture, Sports, Science, and Technology of Japan, and by Health and Labour Sciences Research Grants for Research on Hepatitis and BSE from the Ministry of Health, Labour and Welfare of Japan.

REFERENCES

1. N. Ferry and J. M. Heard. Liver-directed gene transfer vectors. *Hum. Gene Ther.* **9**:1975–1981 (1998).
2. J. Herz and R. D. Gerard. Adenovirus-mediated transfer of low density lipoprotein receptor gene acutely accelerates cholesterol clearance in normal mice. *Proc. Natl. Acad. Sci. USA* **90**:2812–2816 (1993).
3. M. Kaleko, J. V. Garcia, and A. D. Miller. Persistent gene expression after retroviral gene transfer into liver cells *in vivo*. *Hum. Gene Ther.* **2**:27–32 (1991).
4. J. R. Chowdhury, M. Grossman, S. Gupta, N. R. Chowdhury, J. R. Baker, Jr., and J. M. Wilson. Long-term improvement of hypercholesterolemia after *ex vivo* gene therapy in LDLR-deficient rabbits. *Science* **254**:1802–1805 (1991).
5. M. Grossman, S. E. Raper, K. Kozarsky, E. A. Stein, J. F. Engelhardt, D. Muller, P. J. Lupien, and J. M. Wilson. Successful *ex vivo* gene therapy directed to liver in a patient with familial hypercholesterolaemia. *Nature Genet.* **6**:335–341 (1994).
6. M. Nishikawa, S. Takemura, Y. Takakura, and M. Hashida. Targeted delivery of plasmid DNA to hepatocytes *in vivo*: optimization of the pharmacokinetics of plasmid DNA/galactosylated poly(L-lysine) complexes by controlling their physicochemical properties. *J. Pharmacol. Exp. Ther.* **287**:408–415 (1998).
7. M. Hashida, S. Takemura, M. Nishikawa, and Y. Takakura. Targeted delivery of plasmid DNA complexed with galactosylated poly(L-lysine). *J. Control. Release* **53**:301–310 (1998).
8. S. Kawakami, F. Yamashita, M. Nishikawa, Y. Takakura, and M. Hashida. Asialoglycoprotein receptor-mediated gene transfer using novel galactosylated cationic liposomes. *Biochem. Biophys. Res. Commun.* **252**:78–83 (1998).
9. S. Kawakami, S. Fumoto, M. Nishikawa, F. Yamashita, and M. Hashida. *In vivo* delivery to the liver using novel galactosylated cationic liposomes. *Pharm. Res.* **17**:306–313 (2000).
10. J. P. Yang and L. Huang. Overcoming the inhibitory effect of serum on lipofection by increasing the charge ratio of cationic liposome to DNA. *Gene Ther.* **4**:950–960 (1997).
11. S. Li, W. C. Tseng, D. B. Stolz, S. P. Wu, S. C. Watkins, and L. Huang. Dynamic changes in the characteristics of cationic lipidic vectors after exposure to mouse serum: implications for intravenous lipofection. *Gene Ther.* **6**:585–594 (1999).
12. F. Sakurai, T. Nishioka, H. Saito, T. Baba, A. Okuda, O. Matsumoto, T. Taga, F. Yamashita, Y. Takakura, and M. Hashida. Interaction between DNA–cationic liposome complexes and erythrocytes is an important factor in systemic gene transfer via the intravenous route in mice: the role of the neutral helper lipid. *Gene Ther.* **8**:677–686 (2001).
13. K. Kawabata, Y. Takakura, and M. Hashida. The fate of plasmid DNA after intravenous injection in mice: involvement of scavenger receptors in its hepatic uptake. *Pharm. Res.* **12**:825–830 (1995).
14. R. I. Mahato, K. Kawabata, T. Nomura, Y. Takakura, and M. Hashida. Physicochemical and pharmacokinetic characteristics of plasmid DNA/cationic liposome complexes. *J. Pharm. Sci.* **84**: 1267–1271 (1995).
15. T. Takagi, M. Hashiguchi, R. I. Mahato, H. Tokuda, Y. Takakura, and M. Hashida. Involvement of specific mechanism in plasmid DNA uptake by mouse peritoneal macrophages. *Biochem. Biophys. Res. Commun.* **245**:729–733 (1998).
16. K. Nishida, C. Tonegawa, T. Kakutani, M. Hashida, and H. Sezaki. Statistical moment analysis of hepatobiliary transport of phenol red in the perfused rat liver. *Pharm. Res.* **6**:140–146 (1989).
17. K. Nishida, K. Mihara, T. Takino, S. Nakane, Y. Takakura, M. Hashida, and H. Sezaki. Hepatic disposition characteristics of electrically charged macromolecules in rat *in vivo* and in the perfused liver. *Pharm. Res.* **8**:437–444 (1991).
18. K. Nishida, Y. Eguchi, T. Takino, Y. Takakura, M. Hashida, and H. Sezaki. Hepatic disposition characteristics of ^{111}In-labeled lactosaminated bovine serum albumin in rats. *Pharm. Res.* **8**:1253–1257 (1991).
19. Y. Yabe, N. Kobayashi, M. Nishikawa, K. Mihara, F. Yamashita, Y. Takakura, and M. Hashida. Pharmacokinetics and preventive effects of targeted catalase derivatives on hydrogen peroxide-induced injury in perfused rat liver. *Pharm. Res.* **19**:1817–1823 (2002).
20. M. Yoshida, R. I. Mahato, K. Kawabata, Y. Takakura, and M. Hashida. Disposition characteristics of plasmid DNA in the single-pass rat liver perfusion system. *Pharm. Res.* **13**:599–603 (1996).
21. Y. K. Song, F. Liu, S. Chu, and D. Liu. Characterization of cationic liposome-mediated gene transfer *in vivo* by intravenous administration. *Hum. Gene Ther.* **8**:1585–1594 (1997).
22. D. J. Hnatowich and W. W. Layne. and Childs RL. The preparation and labeling of DTPA-coupled albumin. *Int. J. Appl. Radiat. Isot.* **33**:327–332 (1982).
23. J. Sambrook. E. F. Fritsch, T. Maniatis. *Molecular Cloning: A Laboratory Manual* 2nd Edition, Cold Spring Harbor Laboratory Press, Plainview, NY, 1989.
24. M. Nishikawa, C. Miyazaki, F. Yamashita, Y. Takakura, and M. Hashida. Galactosylated proteins are recognized by the liver according to the surface density of galactose moieties. *Am. J. Physiol.* **268**:G849–G856 (1995).
25. T. Kakutani, K. Yamaoka, M. Hashida, and H. Sezaki. A new method for assessment of drug disposition in muscle: application of statistical moment theory to local perfusion systems. *J. Pharmacokinet. Biopharm.* **13**:609–631 (1985).
26. K. Yamaoka, T. Nakagawa, and T. Uno. Statistical moments in pharmacokinetics. *J. Pharmacokinet. Biopharm.* **6**:547–558 (1978).
27. Y. Yano, K. Yamaoka, Y. Aoyama, and H. Tanaka. Two-compartment dispersion model for analysis of organ perfusion system of drugs by fast inverse Laplace transform (FILT). *J. Pharmacokinet. Biopharm.* **17**:179–202 (1989).
28. Y. Yano, K. Yamaoka, and H. Tanaka. A nonlinear least squares program, MULTI (FILT), based on fast inverse Laplace transform for microcomputers. *Chem. Pharm. Bull.* **37**:1035–1038 (1989).
29. S. Kawakami, C. Munakata, S. Fumoto, F. Yamashita, and M. Hashida. Novel galactosylated liposomes for hepatocyte-selective targeting of lipophilic drugs. *J. Pharm. Sci.* **90**:105–113 (2001).
30. S. Bjorkerud and G. Bondjers. Endothelial integrity and viability in the aorta of the normal rabbit and rat as evaluated with dye exclusion tests and interference contrast microscopy. *Atherosclerosis* **15**:285–300 (1972).
31. D. T. Connolly, R. R. Townsend, K. Kawaguchi, W. R. Bell, and Y. C. Lee. Binding and endocytosis of cluster glycosides by rabbit hepatocytes. Evidence for a short-circuit pathway that does not lead to degradation. *J. Biol. Chem.* **257**:939–945 (1982).
32. J. Wu, P. Liu, J. L. Zhu, S. Maddukuri, and M. A. Zern. Increased liver uptake of liposomes and improved targeting efficacy by labeling with asialofetuin in rodents. *Hepatology* **27**:772–778 (1998).

33. L. A. Sliedregt, P. C. Rensen, E. T. Rump, P. J. van Santbrink, M. K. Bijsterbosch, A. R. Valentijn, G. A. van der Marel, J. H. van Boom, T. J. van Berkel, and E. A. Biessen. Design and synthesis of novel amphiphilic dendritic galactosides for selective targeting of liposomes to the hepatic asialoglycoprotein receptor. *J. Med. Chem.* **42**:609–618 (1999).
34. R. I. Mahato, Y. Takakura, and M. Hashida. Nonviral vectors for *in vivo* gene delivery: physicochemical and pharmacokinetic considerations. *Crit. Rev. Ther. Drug Carrier Syst.* **14**:133–172 (1997).
35. R. Blomhoff, H. K. Blomhoff, H. Tolleshaug, T. B. Christensen, and T. Berg. Uptake and degradation of bovine testes beta-galactosidase by parenchymal and nonparenchymal rat liver cells. *Int. J. Biochem.* **17**:1321–1328 (1985).
36. D. P. praaning-van Dalen, A. Brouwer, and D. L. Knook. Clearance capacity of rat liver kupffer, endothelial, and parenchymal cells. *Gastroenterology* **81**:1036–1044 (1981).
37. E. Wisse. An electron microscopic study of the fenestrated endothelial lining of rat liver sinusoids. *J. Ultrastruct. Res.* **31**:125–150 (1970).
38. Z. Gatmaitan, L. Varticovski, L. Ling, R. Mikkelsen, A. M. Steffan, and I. M. Arias. Studies on fenestral contraction in rat liver endothelial cells in culture. *Am. J. Pathol.* **148**:2027–2041 (1996).
39. E. Wisse, R. B. de Zanger, K. Charels, P. van der Smissen, and R. S. McCuskey. The liver sieve: considerations concerning the structure and function of endothelial fenestrae, the sinusoidal wall and the space of Disse. *Hepatology* **5**:683–692 (1985).